

ENRAM STSM Report

**STSM Title:** “Applying bird algorithm to weather radar from Germany, France and Switzerland”;

This is the report relative to the Short Term Scientific Mission (STSM) of Dr. **Baptiste Schmid** (Swiss Ornithological Institute, Switzerland) in the COST Action ES1305 (European Network for the Radar surveillance of Animal Movement, ENRAM), under Working Group 1 and 2: Improvement of weather radar data quality and validation of biological-classification algorithms

**Host institution:** Dr. Adriaan Dokter, Institute for Biodiversity and Ecosystem Dynamics, University of Amsterdam, Amsterdam, The Netherlands.

**Date:** 15/02/2016 - 19/02/2016.

## **Introduction**

This STSM aimed to test the application of the algorithm developed to retrieve bird scatters from weather radar stations (Dokter et al. 2011) in order to quantify the spatiotemporal distributions in bird migration over Switzerland. An uneven terrain and the presence of the Alps in Switzerland are particularly interesting to investigate the influence of environmental conditions (terrain and weather) on migratory strategies of birds. In addition to contribution to fundamental research, the use of bird densities retrieved from weather radar station may contribute to forecast of spatiotemporal distribution of important migration events in order to mitigate conflicts with human constructions and activities.

To retrieve information on bird migration, the algorithm uses the standard deviation of linear velocity model to the radial velocity (VRAD). In contrast to rain or insect that normally move at similar velocity, individual birds may strongly differ in their flight direction and speed. Important variations in flight direction and speed imply high standard deviation from the modelled flight parameters. For altitude layers with relatively high standard deviation in VRAD, the algorithm converts the total reflectivity into bird density, assuming a mean reflectivity per bird.

## **Methods**

### *Weather radar data*

We applied the bird algorithm on reflectivity and radial velocity, saved in ODIM-format (hdf5) at 15 minutes time resolution. We used data from three weather radar stations: Montancy (France), Saint-Nizier (France), and Memmingen (Germany) (see Table 1 for detailed characteristics). Data from the French radar station have been provided in ODIM-format (hdf5) by BALTRAD, in agreement with météo-France. The data from the French stations covered three, three-week periods, namely from May 11 to 31 (Montancy and Saint-Nizier), September 1 to 21 (Montancy and Saint-Nizier) and October 5 to 25 2015 (Montancy only). Germany provided test-data from Memmingen covered

ranging from September 9 to October 12 2015. No suitable data (hdf5-files) from weather radars situated in Switzerland are currently available.

### *Vol2Bird-Software configuration*

We used the algorithm as implemented in the program “Vol2Bird” (available on Github <https://github.com/adokter/vol2bird.git>, version 0.2.1).

We restrict the weather radar data from 5 km to 25 km from the radar station to avoid bias in bird density. On the one hand, increasing the maximal detection range increases the surveyed/gate volume dramatically, which smooths out the variability in speeds and directions of single birds, which compromises radial velocity standard deviation as an indicator of bird migration. Secondly, the height of gates increases with distance (for 1° beam angle:  $\tan(2 \cdot \pi / 360) \cdot \text{distance}$ ), but height of the bins used to compute bird densities is kept constant at 200 m. Hence, at large distances, the gate height become larger by several orders of magnitude to the bin height. This leads to loss of altitude resolution. Because of low scanning angle in Saint-Nizier, little information on bird densities can be retrieved above 2800m asl (Fig. 1).

We used the standard configuration of Vol2Bird, specifying the wave length at 5.3 cm, discarding scans with a Nyquist velocity below 20  $\text{m} \cdot \text{s}^{-1}$ . We applied a radial velocity standard deviation threshold of 2  $\text{m} \cdot \text{s}^{-1}$ . To estimate of bird density, used a mean reflectivity per bird (radar cross section of bird = 11  $\text{cm}^2$ ; Dokter et al. 2011).

The detection algorithm produced vertical profile of bird density, and averaged flight speed and flight direction, every 15 minutes at 200 m height intervals.

Table 1: Characteristics of the radar stations (C-band, Doppler) used for the STSM.

Location	Latitude Longitude	Polarisation	Beam width	Range [km]	Frequency [GHz]	Elevation angles		
						Min	Max	Number
<b>Montancy (FR67)</b>	47.37, 7.02	dual	1.1°	256	5.625	0.4°	7°	7
<b>Saint-Nizier (FR58)</b>	46.07, 4.45	single	1.13°	256	5.625	0.4°	4°	5
<b>Memmingen (DL84)</b>	48.04, 9.55	dual	0.9°	180	5.65	0.4°	24°	10

Data source: < <http://www.eumetnet.eu/opera> >

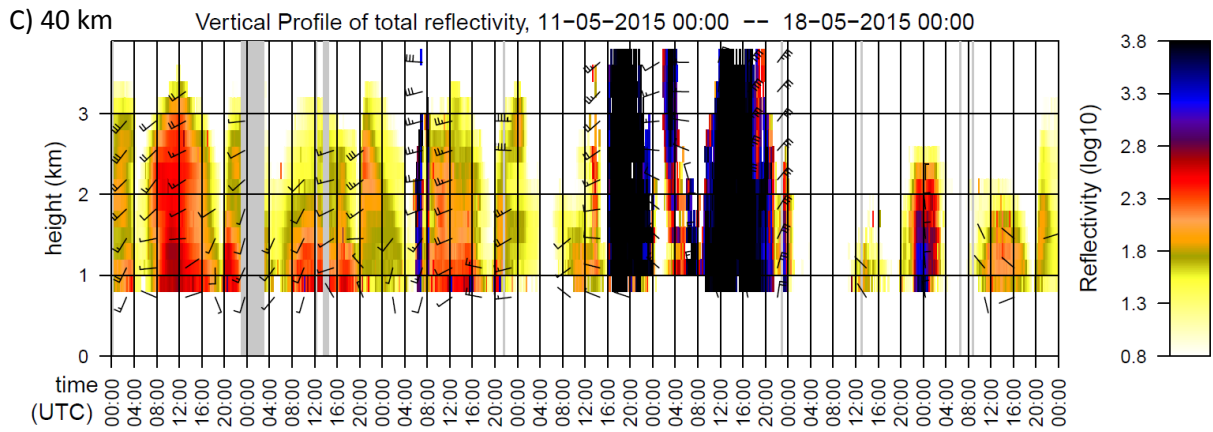
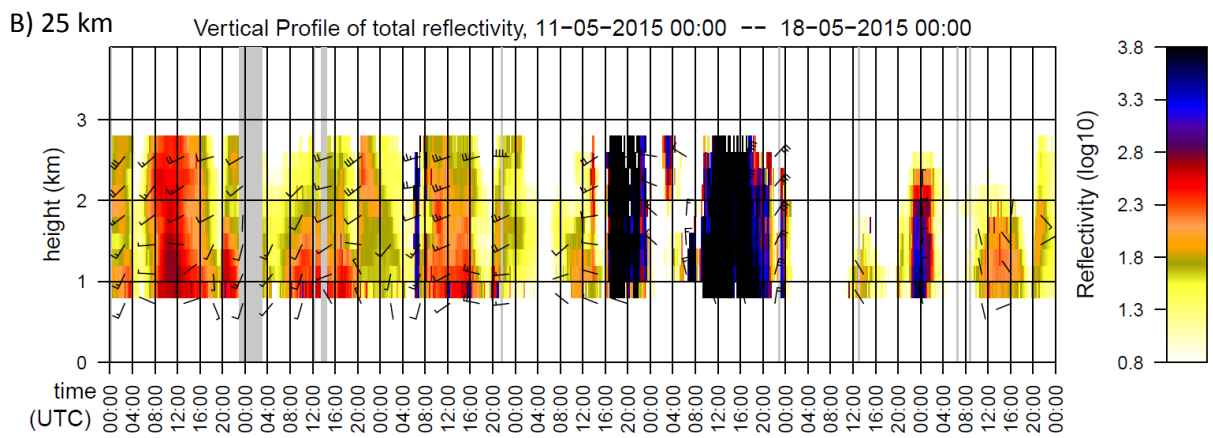
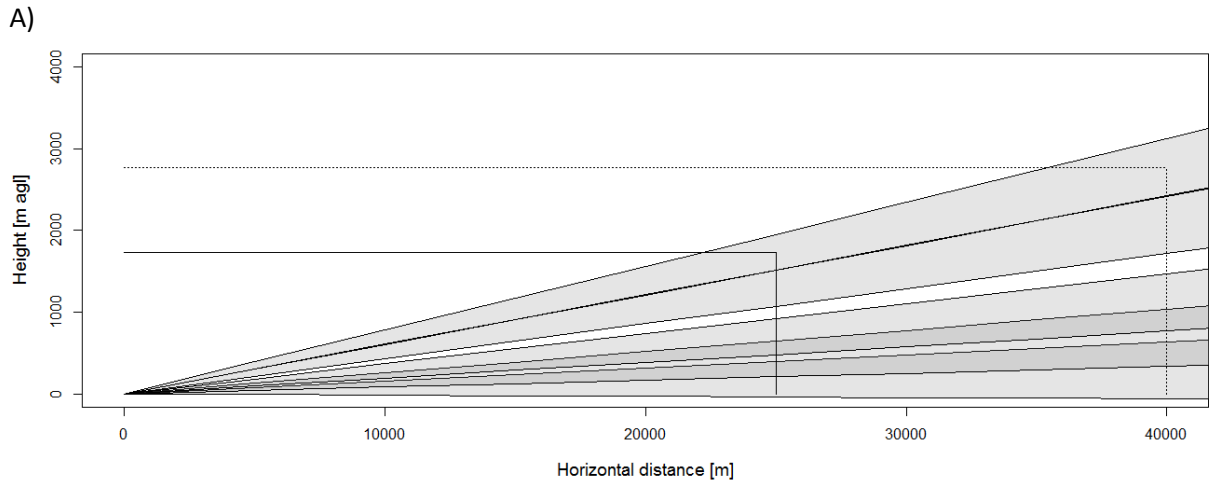


Figure 1: (A) Schematic plot of the beam area for different elevation angles at St-Nizier. The height of the surveyed volume depends on the elevation angles (scan setting: 0.4°, 1.0°, 1.6°, 3.0°, 4.0°; dark grey surfaces represent scan overlap). At 25km distance the highest surveyed altitude is 1734 m agl (continued line), at 40km distance the highest surveyed altitude is 2774 m agl (dotted line). (B) Spatiotemporal distributions of total reflectivity. The range of height distributions of total reflectivity may thus depend on the maximal horizontal distance: B) 25 km and C) 40km. Barbs (panels B and C) depict the mean direction and velocity of the scatters.

## Results and discussion

### *Bird extraction*

The Vol2Bird-algorithm uses primarily the standard deviation of radial velocity (VRAD) from the modelled radial velocity to identify altitude layers dominated by biological scatters. The visualisation of the spatio- (height) and temporal distributions of reflectivity and bird density generally provide the expected pattern. For instance, in many cases, the bird densities increase sharply after dawn (Fig. 2B, Fig. 5B), indicating the mass uplift movements of nocturnal migratory birds.

We use PPI-plots visualise of raw data on reflectivity and VRAD (Fig 3-4, and Fig. 6-7). Important heterogeneity in VRAD is identified as biological scatter (e.g. Fig. 3 and Fig. 7). Highly homogenised VRAD is then identified as rain (2015.10.10 at 19:00 in Fig. 2B, for data showed in Fig. 4).

The examination of the spatiotemporal distributions (Fig. 5B) reveals only few unsatisfactory performance of the algorithm to remove rain scatters, and require further improvement to distinguish birds from insects. The remaining non-animal scatters may arise due to radar-specific settings or to particular meteorological events. Insect contamination is probably most important during day-time and warm seasons.

### *Ground clutter and rain filter*

The algorithm successfully filters out the ground clutter (Fig 2, Fig 5) but the algorithm output also remain slightly contaminated by rain (Fig. 5). This is particularly the case for the weather radar station of Montancy and St-Nizier (France). Indeed, the remaining unfiltered rain probably originates from the small areas with highly heterogeneous radial velocity (Fig. 7). The difficulty to efficiently filter rain from the French radar system might be due to particular triple-PRT scheme used to record the radial velocity.

### *Insect scatters*

The proportion of insects of the algorithm output may be particularly important during day-time and during the warm seasons (Fig. 1, between 8:00 and 16:00; Fig. 8). Because of higher temperature and seasonal emergence of insects, it is most likely to observe insects together with migratory birds in late spring, summer and early autumn. Insects and birds differ in their flying capability. For instance, the averaged ground speed of flying insects (< 5 m/s) is generally lower than the ground speed of birds (8-10 m/s). While differences in speed may allow to differentiate insects from birds (e.g. Rosa et al 2015), wind conditions can also strongly influence ground speed of birds (Fig. 9).

The algorithm extracts high number of low-velocity scatters in May (Fig. 10 and Fig. 11). These are unlikely to be birds (slow speed, less diurnal bird migration in May than in March and in April). The passive flight of insects in the wind flows largely homogenise the VRAD and insect are normally filtered out by the Vol2Bird algorithm. However, specific triple-PRT (pulse repetition time) used by French weather radar system (Tabary et al 2006) may create noise in the radial velocity data that increase the standard deviation of the VARD. Unless the scatter show flight direction in opposite

direction as the wind profile (birds flying in head wind), French data from late spring to early autumn are likely to be contaminated by insects.

## Conclusion

During the STSM in Amsterdam I have learnt to process raw weather radar data (hdf5-format) using the Vol2Bird-software. The generated algorithm outputs clearly identify peaks of bird migrations. To date, it remains nonetheless difficult to process a wide range of weather radar data. On the one hand, unfiltered hdf5-files are not yet readily available to the OPERA (or BALTRAD) network from all countries. On the other hand, the data processed during the STSM also highlight the need to either carefully select the time period, or to manually validate the data in order to avoid remaining rain scatters and insect contamination. Radar system using dual-polarisation may offer further opportunities to better distinguish insects from bird scatters. Albeit from these specific issues, the results presented here are promising for upcoming research projects on bird migration.

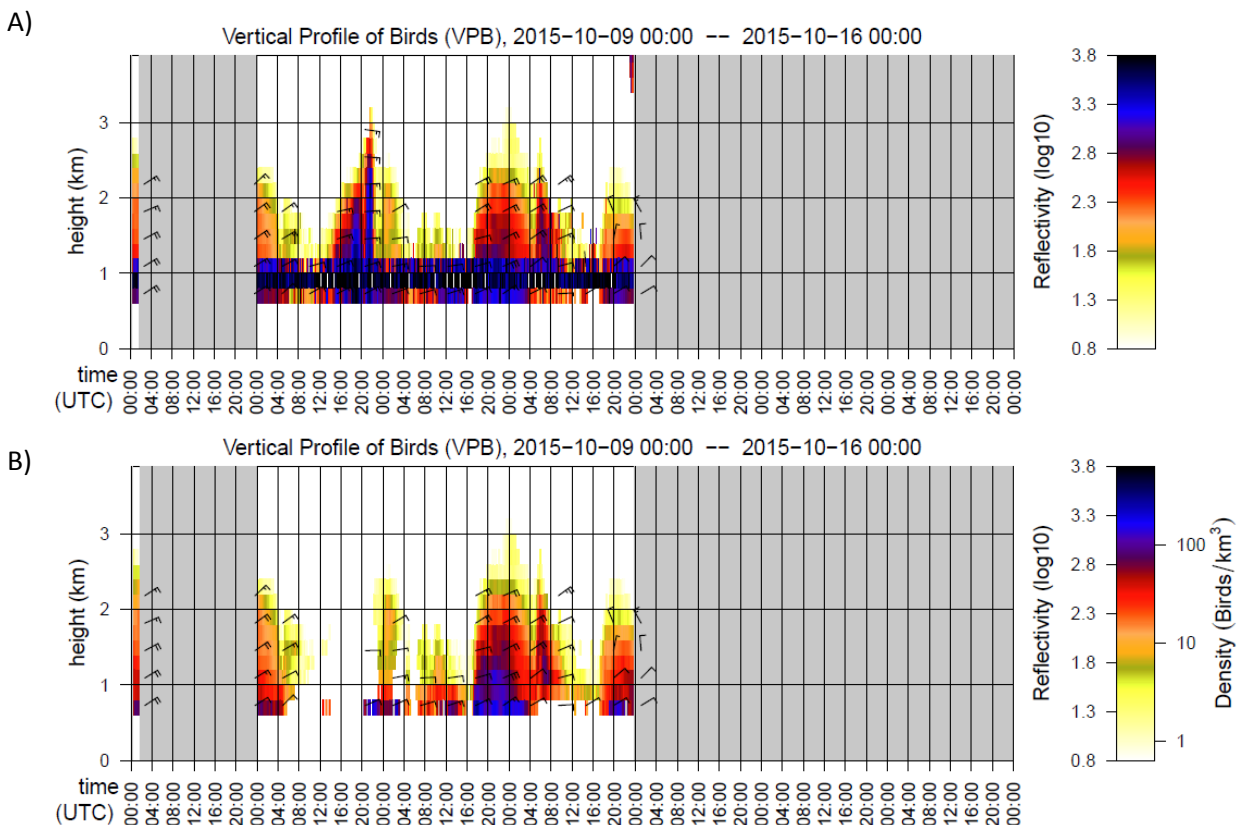


Figure 2: Spatiotemporal distribution in Memmingen of (A) total reflectivity and (B) reflectivity of biological scatter (as produced by the Vol2Bird algorithm for data displayed in A). Barbs (panels A and B) depict the mean direction and velocity of the scatters. Missing data are represented in grey.

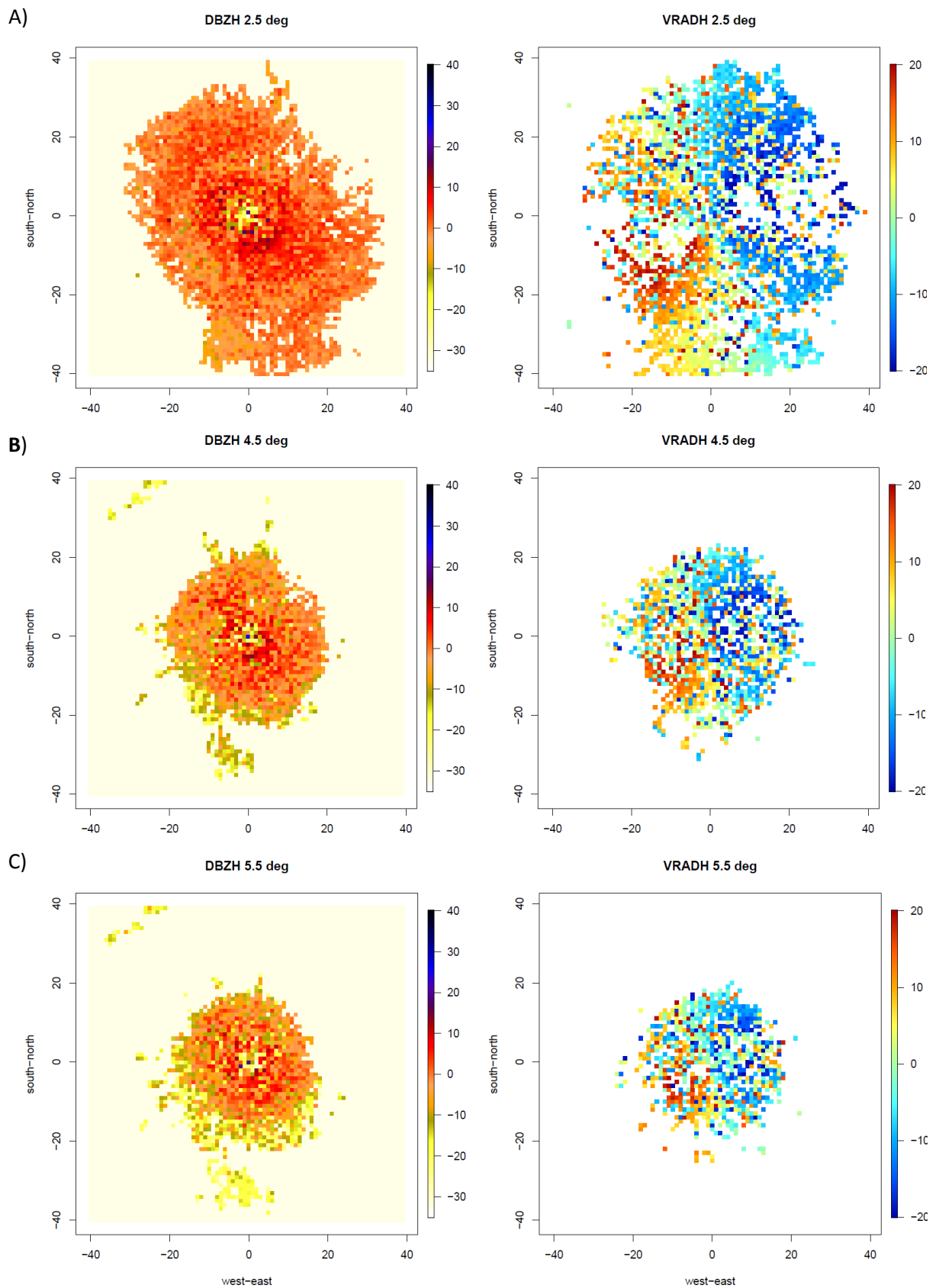


Figure 3: PPI-plots of (left) total reflectivity [DBZH] and (right) radial velocity [VRADH] used to identify biological scatters that show heterogeneous radial velocity at Memmingen on 2015-10-11 21:00 (see corresponding time in Fig. 2), for A) elevation angle 2.5°, B) elevation angle 4.5°, and C) elevation angle 5.5°.

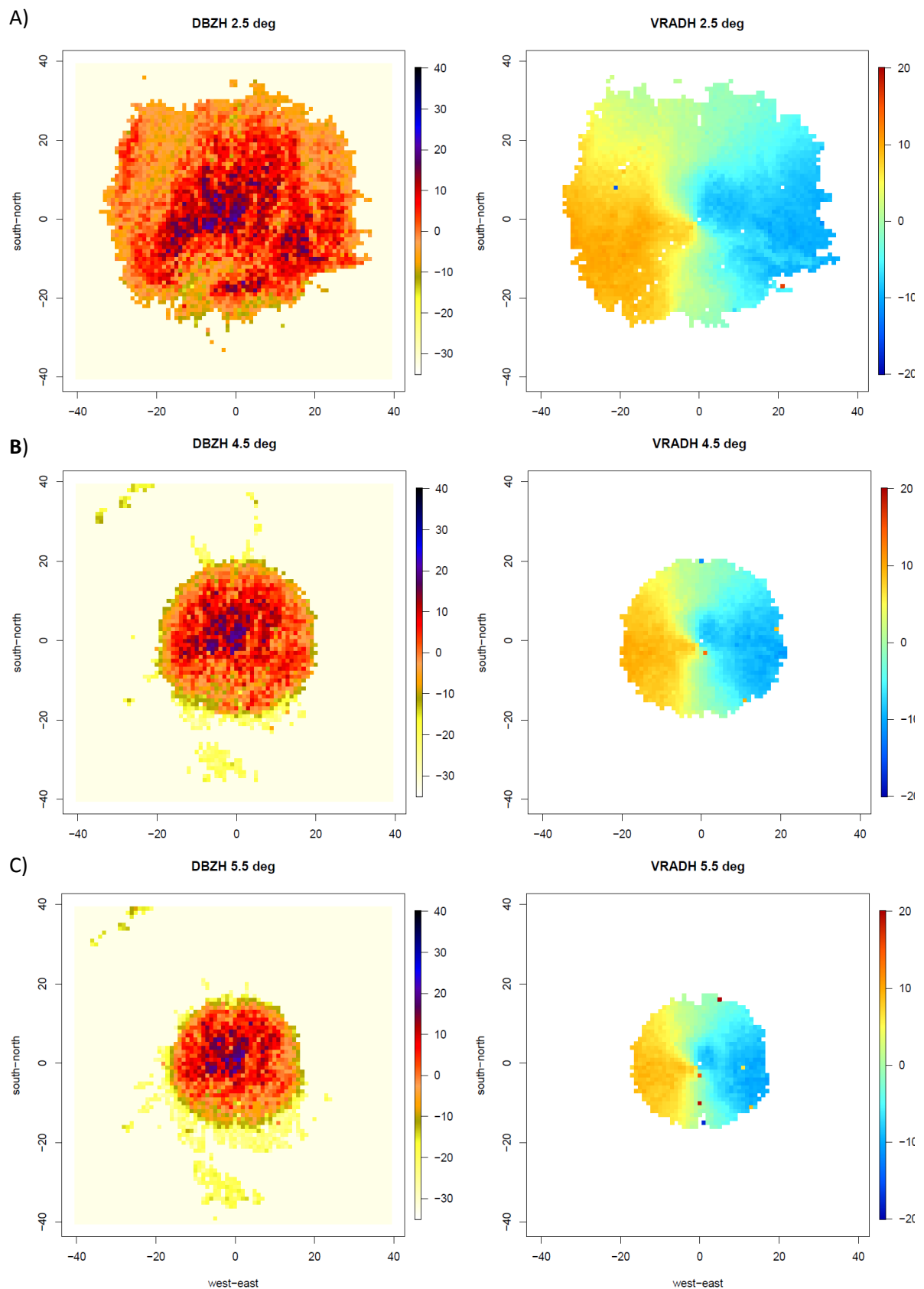


Figure 4: PPI-plots of (left) total reflectivity [DBZH] and (right) radial velocity [VRAD] used to identify rain scatters that show homogeneous radial velocity at Memmingen on 2015-10-10 19:00 (see corresponding time in Fig. 2), for A) elevation angle 2.5°, B) elevation angle 4.5°, and C) elevation angle 5.5°.

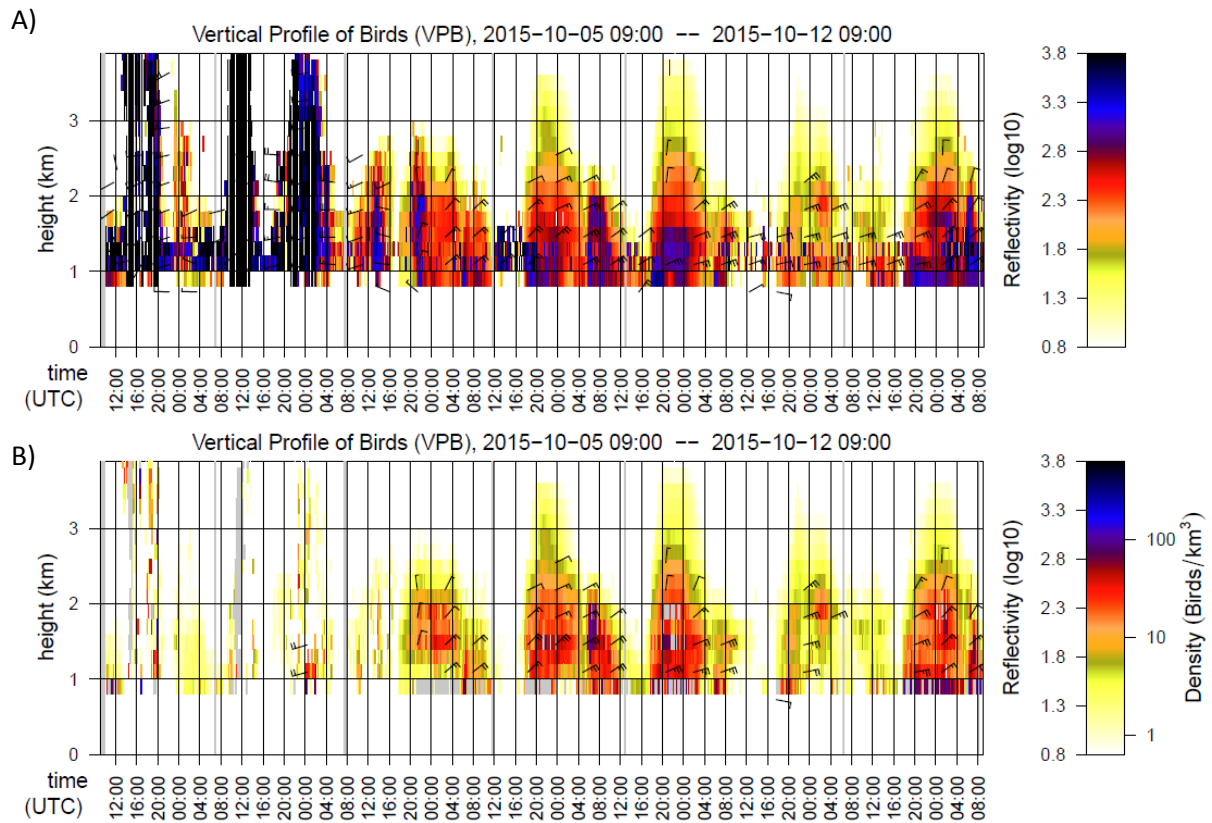


Figure 5: Spatiotemporal distribution in Montancy of (A) total reflectivity and (B) reflectivity of biological scatter only (output of the Vol2Bird-algorithm) for the same raw data as in (A). Ground clutter (1000 – 1400 m asl in panel A) is efficiently removed by the algorithm, and the output data remain only slightly contaminated by rain (see October 5 – 6). Barbs (panels A and B) depict the mean direction and velocity of the scatters.



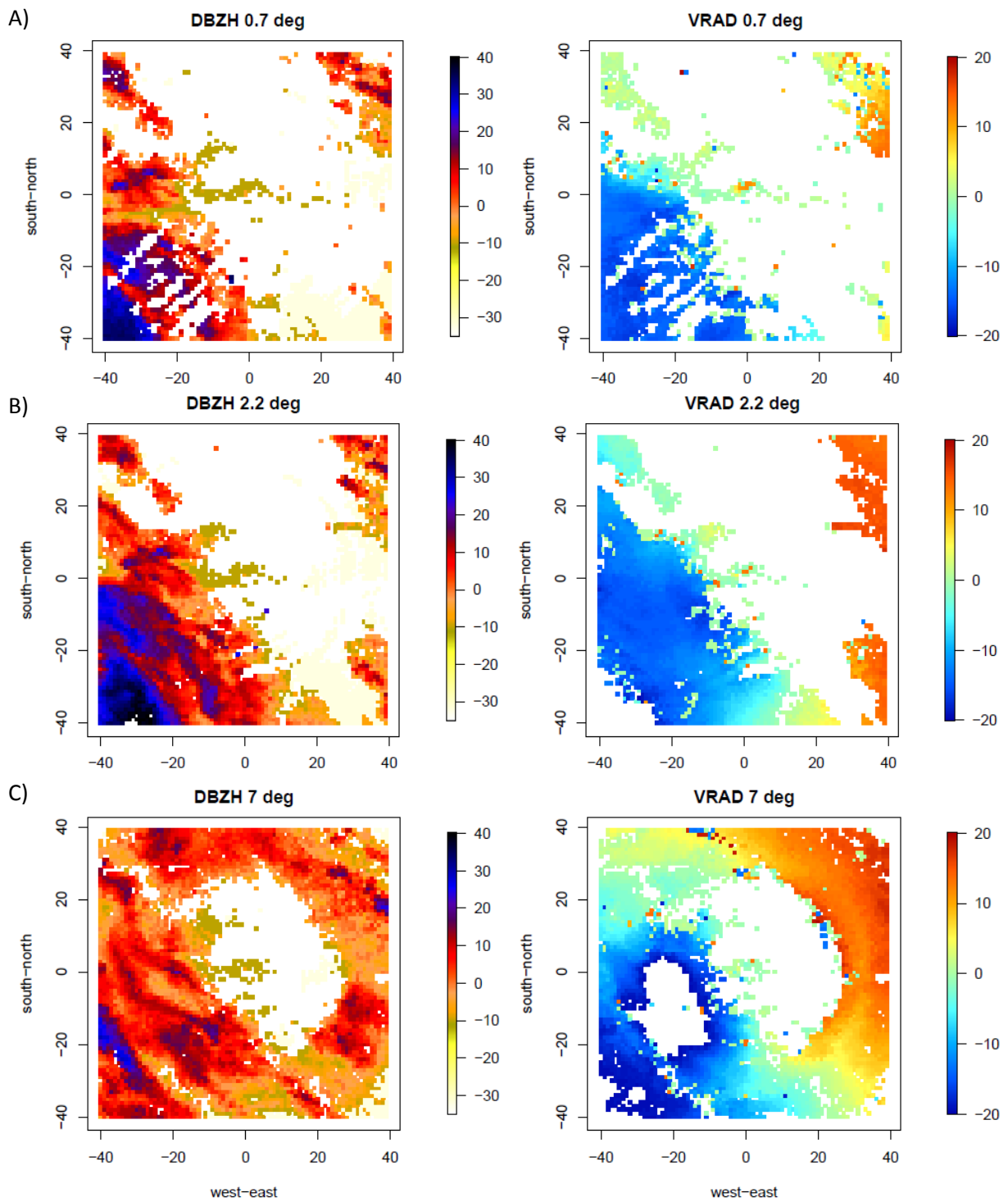


Figure 6: PPI-plots of (left) total reflectivity [DBZH] and (right) radial velocity [VRAD]. The scatters are identified as rain due to the largely homogeneous radial velocity: (A) Montancy, 2015-10-05 16:00, elevation 0.7°; (B) Montancy, 2015-10-05 19:45, elevation angle 2.2°; (C) Montancy, 2015-10-05 19:45, elevation angle 7.0° (see corresponding time in Fig. 5).

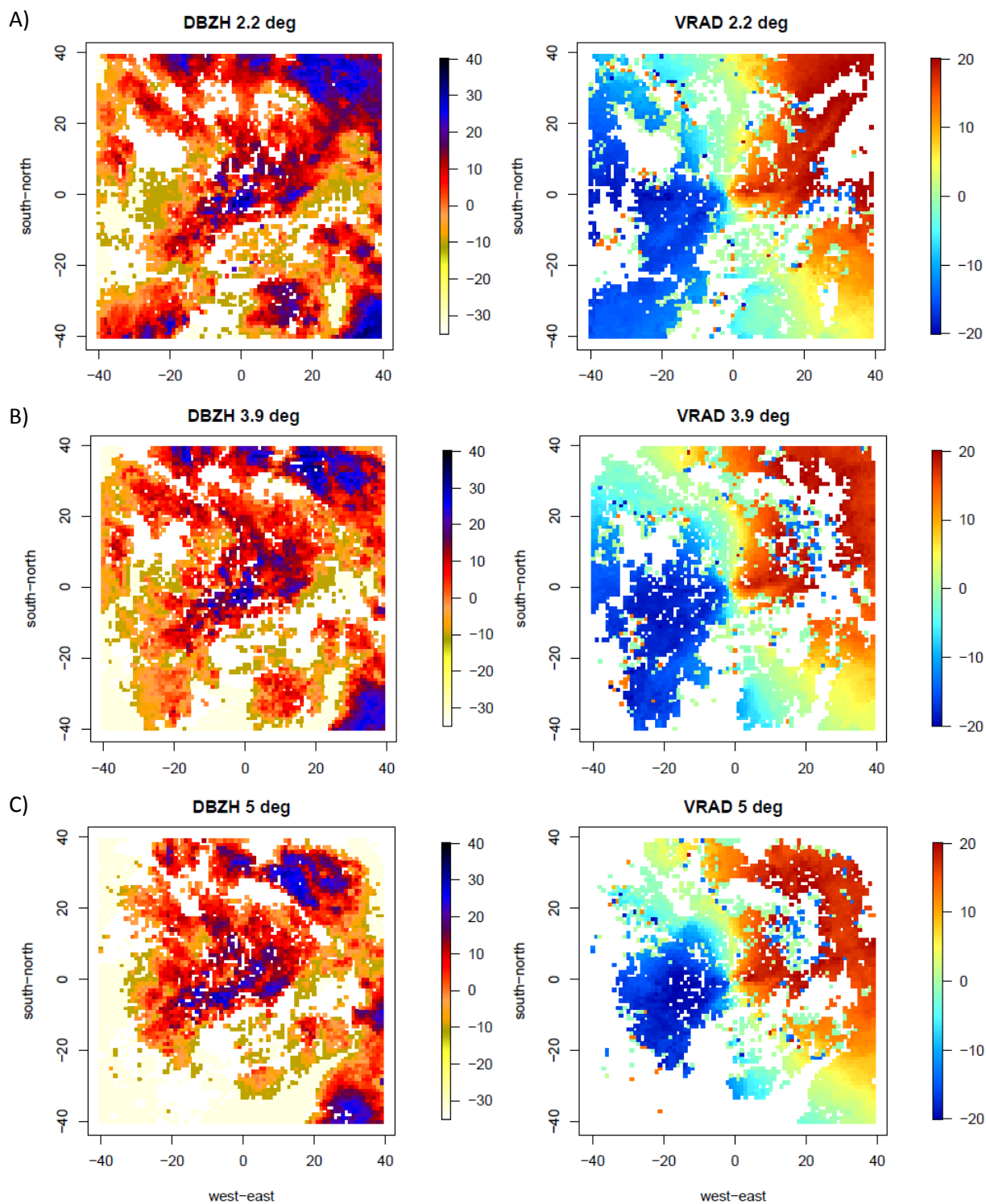


Figure 7: PPI-plots of (left) total reflectivity [DBZH] and (right) radial velocity [VRAD]. The scatters are identified as biological scatters due to the heterogeneous radial velocity: (A) Montancy, 2015-10-05 19:15, elevation  $0.7^\circ$ ; (B) Montancy, 2015-10-05 19:45, elevation angle  $2.2^\circ$ ; (C) Montancy, 2015-10-05 19:45, elevation angle  $7.0^\circ$  (see corresponding time in Fig. 5).

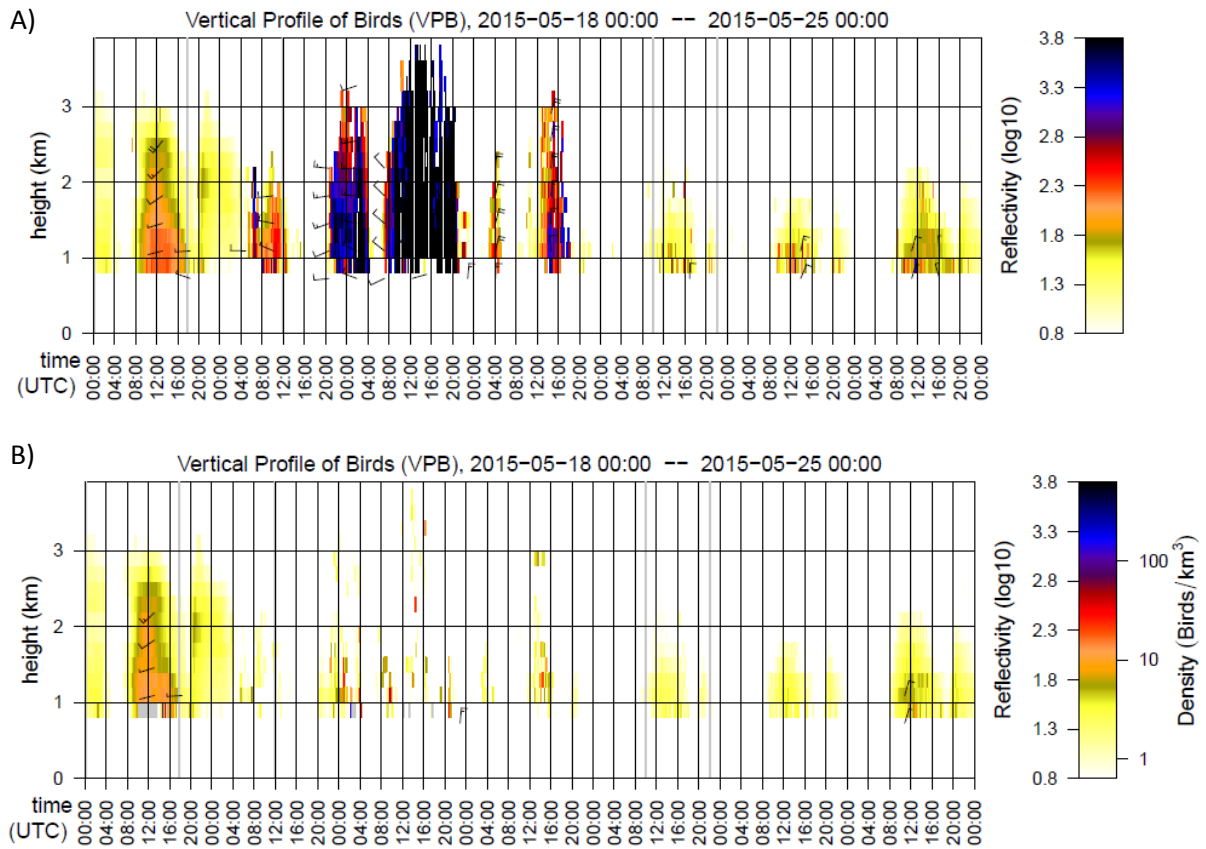


Figure 8: Spatiotemporal distribution in Saint-Nizier of (A) total reflectivity and (B) reflectivity of biological scatter only (output of the Vol2Bird-algorithm) for the same raw data as in (A). The output data remain only slightly contaminated by rain (see May 20). Barbs (panels A and B) depict the mean direction and velocity of the scatters.

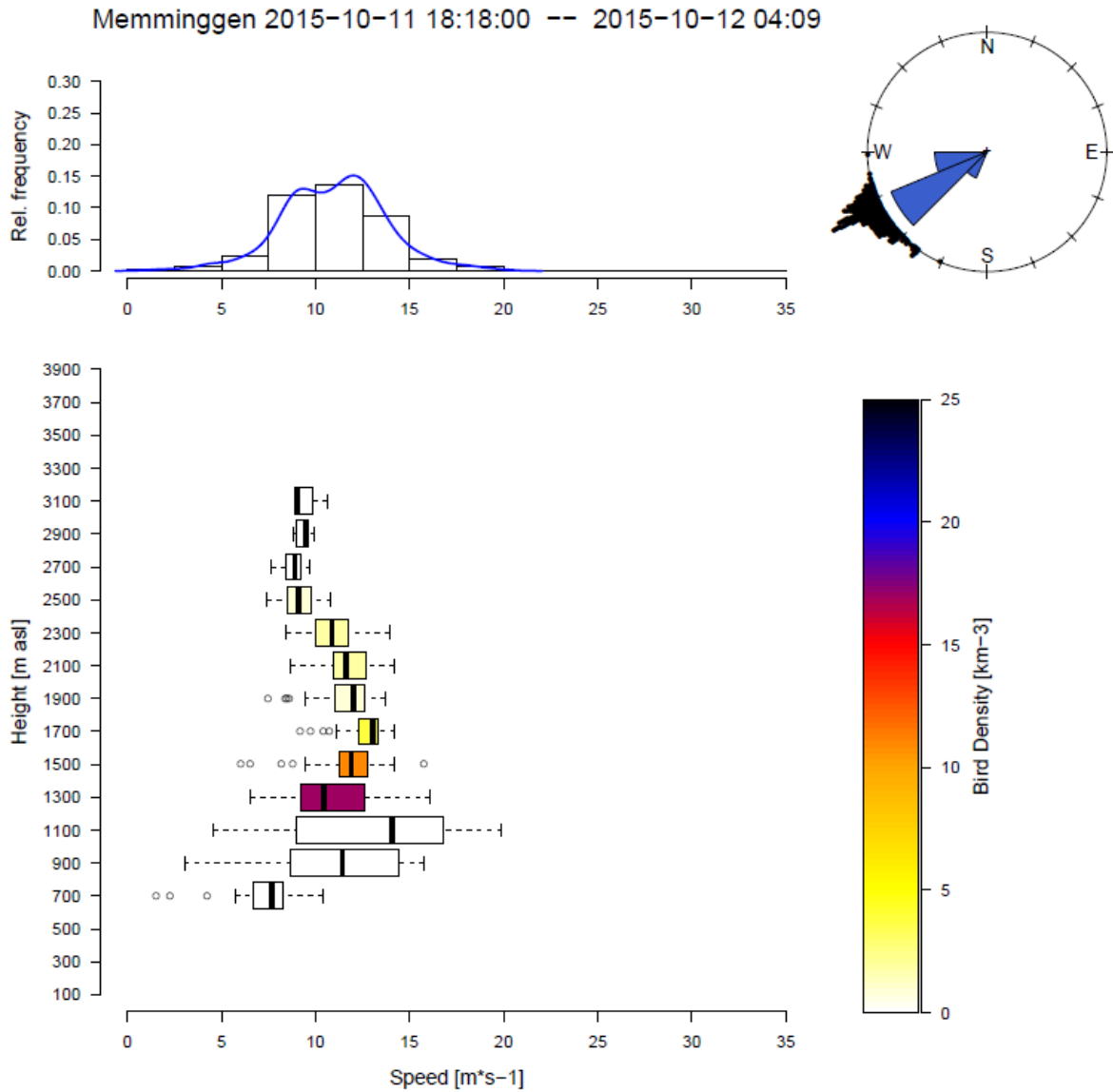


Figure 9: Relative frequency distributions of flight speed (top left) and height distribution of flight speed (bottom, colours indicate the bird density), and the distributions of flight directions, for nocturnal migration at Memmingen (see corresponding time in Fig. 2).

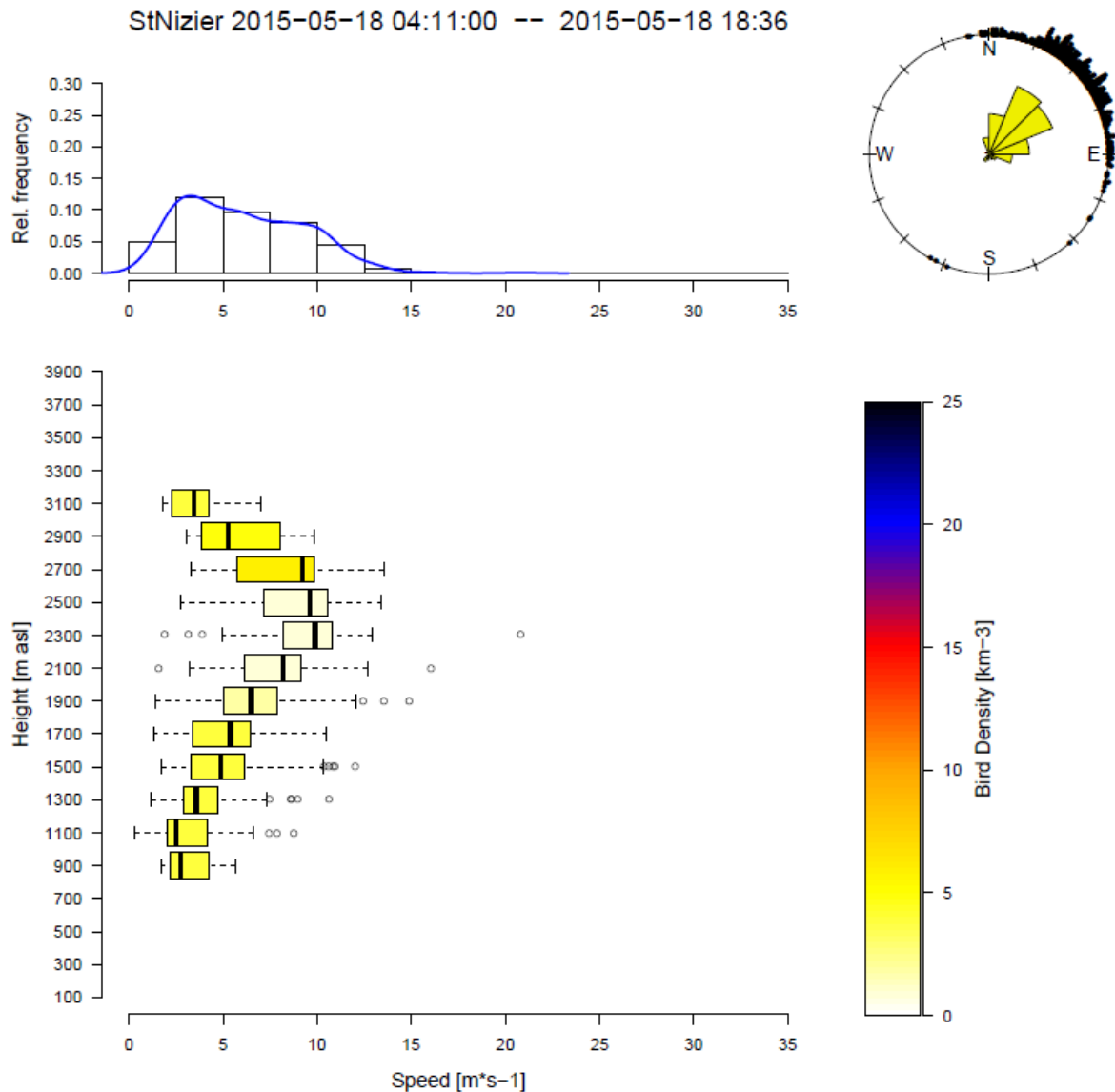


Figure 10: Relative frequency distributions of flight speed (top left) and height distribution of flight speed (bottom, colours indicate the averaged bird density), and the distributions of flight directions, for diurnal migration at Saint-Nizier (see corresponding time in Fig. 8).

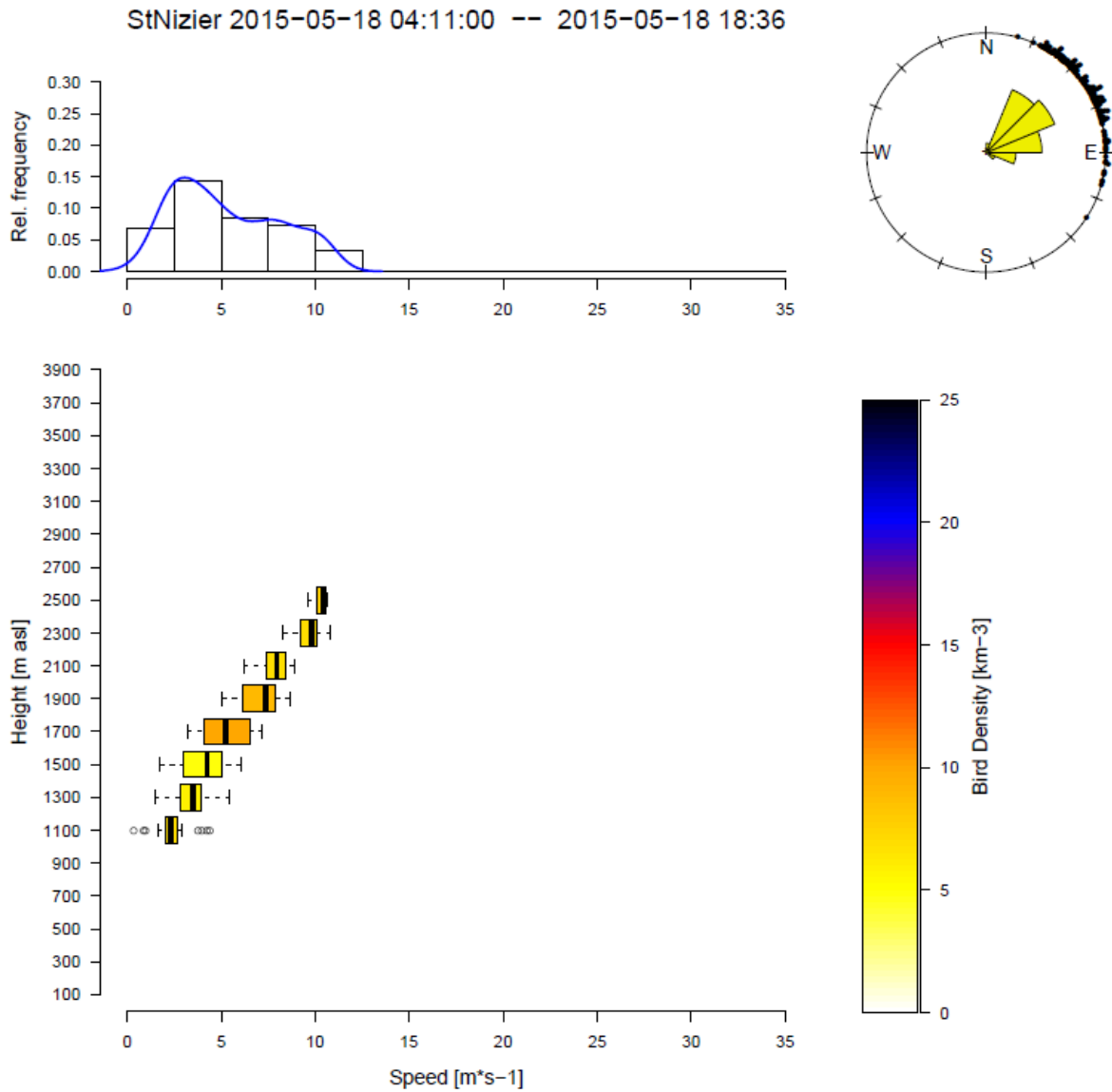


Figure 11: Same as Fig. 10. To reduce the possible influence of insect scatters, we used bird density threshold of 5 birds/km<sup>3</sup> and speed standard deviation of 2 m/s on the data.

## Acknowledgements

I thank Günther Haase (SMHI), Klaus Stephan (DWD), and Météo France for providing the data. I also thank Adriaan Dokter, and Judy Shamon-Baranes and her working group at UVA for their hospitality. Many thanks to Jason Chapman, Suzannah Chapman and Silke Bauer for the coordination of the STSMs of ENRAM. This STSM is a financially approved E-Cost action (ES1305).

## References

Dokter A.M., Liechti F., Stark H., Delobbe L., Tabary P., Holleman I. (2011) *Bird migration flight altitudes studied by a network of operational weather radars*. J. R. Soc. Interface, **8**, 30–43. DOI: [10.1098/rsif.2010.0116](https://doi.org/10.1098/rsif.2010.0116)

Rosa I.M.D., Marques A.T., Palminha G., Costa H., Mascarenhas M., Fonseca C., Bernardino J. (2015) Classification success of six machine learning algorithms in radar ornithology. *Ibis*, online early. doi: 10.1111/ibi.12333.

Tabary P., Guibert F., Perier L., Parent-du-Chatelet J. (2006) *An operational triple-PRT Doppler scheme for the French radar network*. J. Atmospheric and Oceanic Technology, **23**, 1645-1656 DOI: [10.1175/JTECH1923.1](https://doi.org/10.1175/JTECH1923.1)